GASFLOW validation with Panda tests from the OECD SETH Benchmark covering steam/air and steam/helium/air mixtures

Peter Royl, John R. Travis, Wolfgang Breitung
Forschungszentrum Karlsruhe
Intitut für Kern- und Energietechnik
76021 Karlsruhe, Germany

Jongtae Kim, Sang Baik Kim,
Korean Atomic Energy Research Institute
Division of thermal-hydraulics and safety research
Yseong,Daejeon
305-353 Korea

ABSTRACT

The CFD code GASFLOW solves the time-dependent compressible Navier-Stokes Equations with multiple gas species. GASFLOW was developed for non nuclear and nuclear application. The major nuclear applications of GASFLOW are 3D analyses of steam/hydrogen distributions in complex PWR containment buildings to simulate scenarios of beyond design basis accidents. Validation of GASFLOW has been a continuously ongoing process together with the development of this code. This contribution reports the results from the open post test GASFLOW calculations, that have been performed for new experiments from the OECD SETH Benchmark. Discussed are the steam distribution tests 9 and 9bis , 21 and 21bis involving comparable sequences with and without steam condensation and the last SETH test 25 with steam/Helium release and condensation. The latter one involves lighter gas mixture sources like they can result in real accidents. The Helium is taken as simulant for hydrogen.

1. INTRODUCTION

The CFD code GASFLOW II solves the time-dependent compressible Navier-Stokes Equations with multiple gas species (Travis et al., 2007). It models two-phase effects of condensation and/or vaporization in the fluid mixture region with the assumption of the homogeneous equilibrium (HEM) model, two phase heat transfer to and from walls and internal structures by convection and mass diffusion, and the chemical kinetics of hydrogen combustion with general ignitor models and catalytic recombination. The code is applied in the 3D analysis of steam/hydrogen distribution in various PWR containments to simulate scenarios of beyond design basis accidents. Validation of GASFLOW with thermal hydraulic experiments that simulate such scenarios or some of their aspects is an ongoing effort with involvement of all members of the GASFLOW users group, which comprises industrial and research partners. GASFLOW successfully participated in the blind and in the open post test analysis of the international standard problem ISP47. The success and the problems in simulating the ThAI test TH13 from this benchmark have been shown in a paper to the previous CFD4NRS conference (Royl et al., 2006). The OECD Panda SETH experiments and their results, which are accessible to members of the funding countries, have further widened the data base for predicting such containment related severe accident scenarios. The tests were designed by the Swiss Paul Scherrer Instiute and performed in their Panda facility (Auban et al, 2006). A GASFLOW analysis of some of these tests has been jointly made by the Korean Atomic Energy Research Institute (KAERI) and by Forschungszentrum Karlsruhe. This contribution will report the results from the open post test GASFLOW calculations, that have been performed for the steam distribution tests 9 and 9bis, 21 and 21bis involving comparable sequences without and with steam condensation and for the latest Panda SETH test 25 with

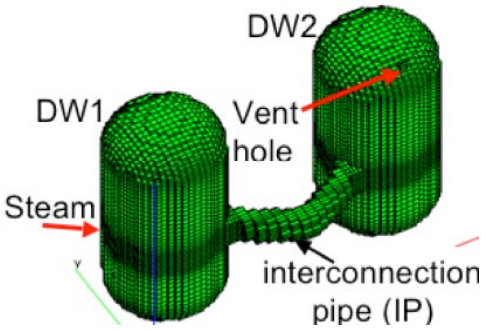

Fig. 1: Fine 3D model of the Panda facility

steam/Helium release and condensation. The latter one involves lighter gas mixture sources like they can result in real accidents. The Helium is taken as the simulant for hydrogen. Figure 1 shows one of the 3D cartesian GASFLOW facility models applied in the analysis of these tests.

2. SIMULATED PANDA SETH TESTS

The OECD SETH project has initiated a series of 25 tests in the two rooms DW1 and DW2 of the large scale thermal hydraulic facility Panda to simulate mixing and stratification phenomena in a larger multi-compartment gas volume approaching the dimension of actual containment compartments. Figure 2 gives an overview of the 6 experiments from this series that were simulated with GASFLOW. The two vessels

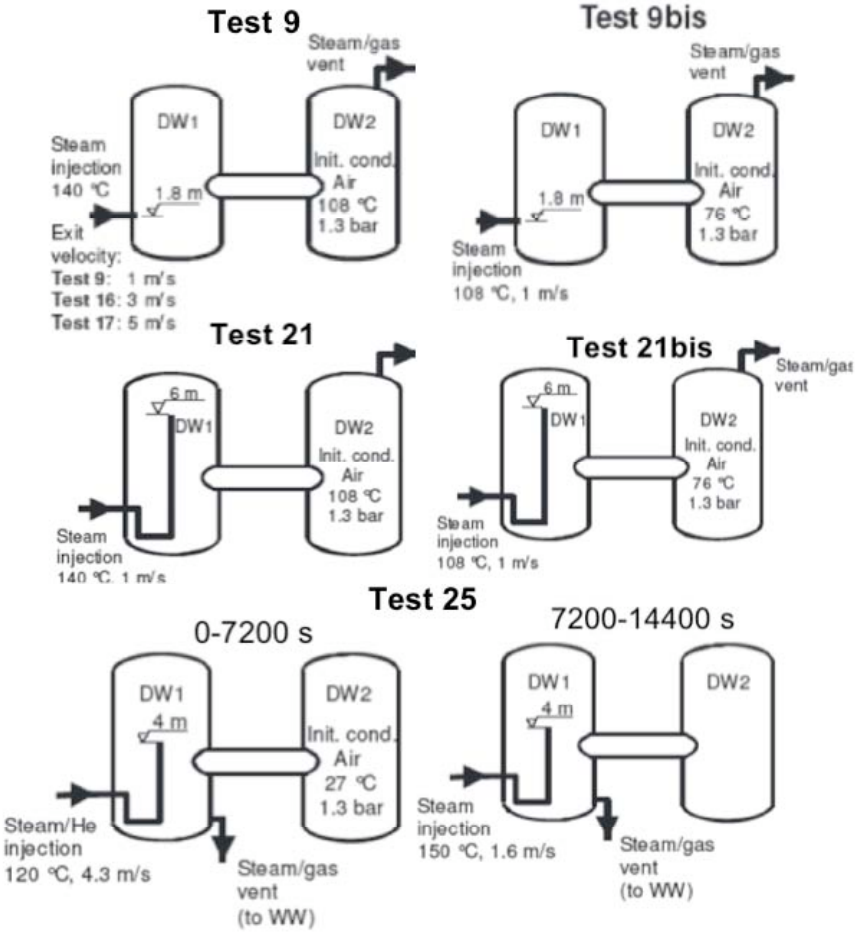

Fig. 2: SETH tests analyzed with GASFLOW

DW1 and DW2 have the same volume of 90 m3 each and are all initially filled with dry air. A feeding vessel DW1 is connected to the receiving vessel DW2 through a bended pipe with a large diameter. In all analyzed tests except test 25 a vent hole was active in the dome of DW2 that maintained a constant pressure of 1.3 bar. Tests 9 and 9bis investigated the spreading of a buoyant steam plume over these two compartments that resulted from a low velocity horizontal injection into the lower region of DW1. Tests 21 and 21bis investigated the spreading from an axial steam injection high in the dome of DW1. Tests 9 and 21 were run

from an axial steam injection high in the dome of DW1. Tests 9 and 21 were run with higher steam temperatures. The whole facility was preheated to a high enough temperature to suppress steam condensation. Tests 9bis and 21bis were run in a less pre heated facility with a lower steam temperature that allowed for steam condensation. The 9 and 21 series tests all applied the same constant rate of steam injection of 14g/s. They are well suited for testing condensation models currently implemented in CFD codes. The test facility is insulated but can absorb heat with its heat capacity. Test 25 is the final test from the SETH series. It simulated a sequence of steam/helium injections into the air filled facility initially at room temperature (Paladino, 2007). The gas spreads into a dead end vessel DW2 because the vent valve in DW2 is closed. Gas venting in test 25 occurs through a vent pipe in DW1 below the source and interconnecting pipe. This vent pipe connects to the large wet well volume (WW). The vent pressure in this test is recorded. It rises monotonically with time and can be applied as a pressure boundary condition in the analysis instead of the constant vent pressure in DW2. In test 25 only the pressure but not the volume flow rates at the entrance to the vent pipe could be measured. The problem times to analyze the 9 and 21 series tests were 7000s. Test 25 involved two equally long phases of 7200 with a steam/helium injection in phase 1 followed by a pure steam injection in phase 2. The total problem time to analyze for this test is 14400s.

3. GASFLOW MODELS OF THE TEST FACILITY

The facility has been simulated in coarse (13,000), fine (115,000) and extremely fine (365,000) 3D Cartesian meshes (figure 3). A fine mesh with 115,351 cells was developed with a smaller number of blocked cells (orientation I). The source had to be split up into equal x and y components with this mesh to achieve the proper injection angle of 45 degrees because the steam injection was not on the x-coordinate axis. The coarse model for orientation II simulated the injection along the x-axis. It had 24,180 cells with nearly equidistant xyz meshes of 33 cm and a higher fraction of blocked cells. The finest grid model for orientation II had 365,040 cells with fine axial grid sizes of 5 cm between the injection location and the horizontal sensor plane at 380 cm and fine xy mesh of 5cm on the source side of DW1. Good agreement with the test data was found with all meshes. Comparisons showed that neglecting the bend of the connection pipe and modeling a straight pipe with a length of 5m between the vessels has no strong impact on the results. To economize on the CPU time we then ran most tests with the straight pipe model which allows to simulate the tests with only 13,182 cells of nearly equidistant meshes of 33.33 cm. For the studied tests, coarse and fine meshes gave quite good overall results as long as condensation didn't come into play. With condensation we obtained nearly mesh independent overall results when the heat transfer with the applied wall functions was enhanced in the ratio of the

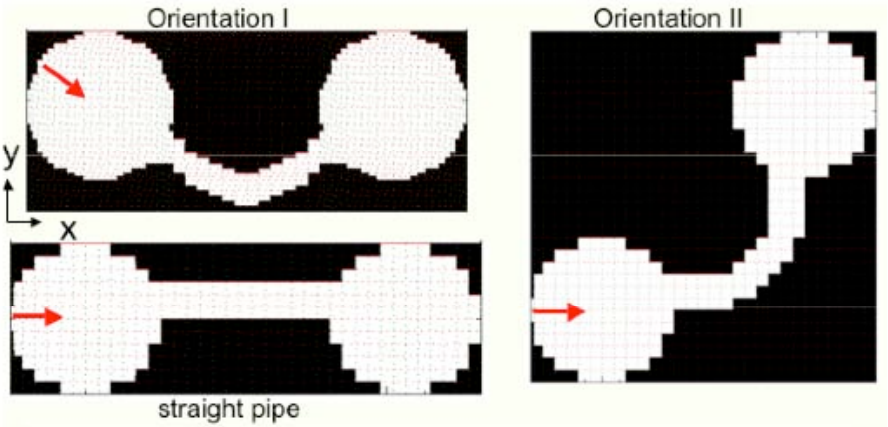

Mesh	Orientation	Cells
coarse	I	15,392
	II	24,180
	straight pipe	13,182
fine	I	115,351
finest	II	365,040

Fig. 3: Applied horizontal meshes

coarse and fine wall mesh. Analysis of test TH13 from ISP47 showed a similar agreement when going from a fine to a coarse mesh with this type of wall function adjustment. The large fraction of structure surfaces in the facility that have mostly stagnant flow conditions during the test justifies this enhancement. Like in all other CFD codes that apply wall functions to avoid resolving the boundary layer there is still a need for a wall function formulation that gives a mesh independent heat transfer in the transition to stagnant flow conditions. Table 1 gives an overview of the analyzed tests, the key test parameters and the applied meshes. All simulations applied the second order van Leer advection scheme together with the standard k-ε turbulence model.

Table 1: SETH test parameters and GASFLOW facility models

test	T0 vessel [C]	Model	steam source [g/s]	Helium source g/s	inj. velocity [m/s]	steam Temp. [C]	Steam conden-sation	Problem Time [s]
9	108	coarse	14	-	1	140	no	7000
		str. pipe						7000
		fine						4000
		finest						250
9bis	76	coarse	14	-	1	108	yes	7000
		str. pipe						7000
		fine						4000
		finest						250
21	108	str. pipe	14	-	1	140	no	7000
21bis	76	str. pipe	14	-	1	108	yes	7000
25	27	str. pipe	64	8	4.3	120	yes	14400

4. RESULTS

4.1 Tests 9 and 9bis

The fine and finest mesh simulations of these tests all adapted the mesh to make the faces of the feeding cells for the horizontal buoyant plume to match the area of the injection orifice to inject the steam with its correct injection momentum. In test 9 with the finest mesh the horizontal temperature profile 2m above the injection location (figure 4) shows the same location and height of the peak at 250 s as the CFX-4 simulation with the finest mesh of 700,000 cells. Calculations with a coarse GOTHIC model with 26,000 cells give about the same peak location but lower peak temperatures (Andreani, 2005). The coarse mesh GASFLOW model injects with a too low injection momentum and gives the peak closer to the wall with similar peak

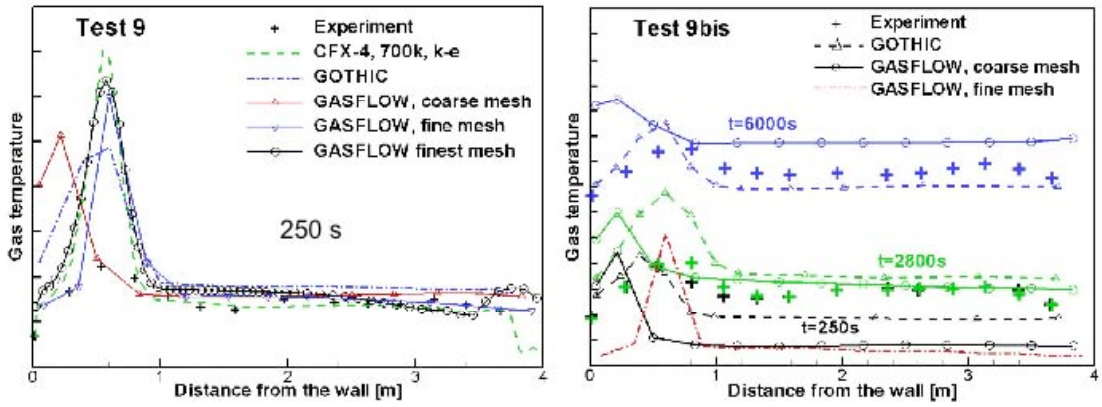

Fig. 4: Horizontal temperature profiles 2 m above injection jet

temperatures as GOTHIC. More mixing of the momentum, mass, and energy occurs in the coarser mesh. So far all CFD analyses of test 9 predict higher than measured peak temperatures at the comparison point. The reasons for this are not yet understood. Condensation

doesn't effect modeling of test 9 in any calculation. Some influence could come from radiation cooling of the hotter steam plume which was not accounted for in any calculation. The measured temperature peaks from test 9bis at 250s are better predicted. Over predictions are again seen around 2800 and 6000s. The tail values outside the peak are in better agreement than the peaks.

In the early test phase the results with the fine and coarse mesh showed significant differences in the velocity profiles. But these did not alter the overall convective flow between the two test vessels, because local mesh effects generally smeared out during the deflection of the buoyant flow in the dome region. The axial profiles of the steam concentrations along the centerline of DW1 and DW2 (figure 5) show acceptable agreements with the test data. The

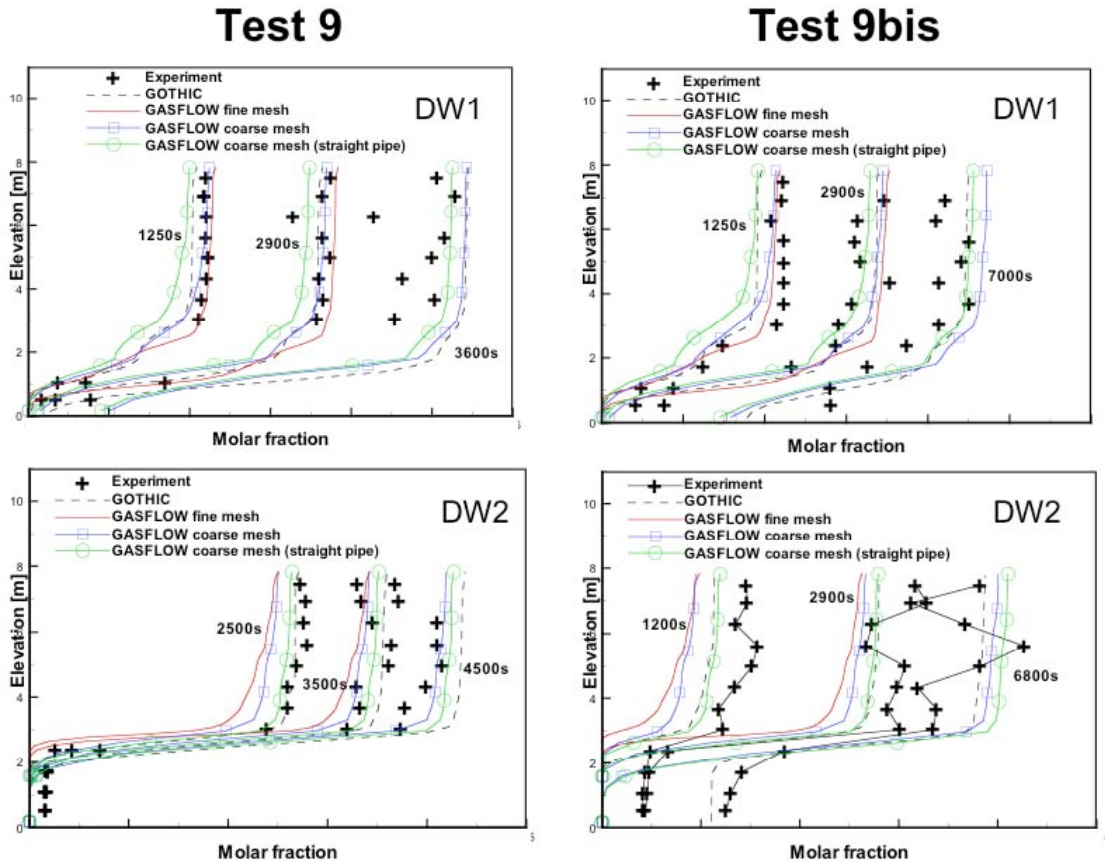

Fig. 5: Axial steam concentration profiles in the centerlines of DW1 and DW2

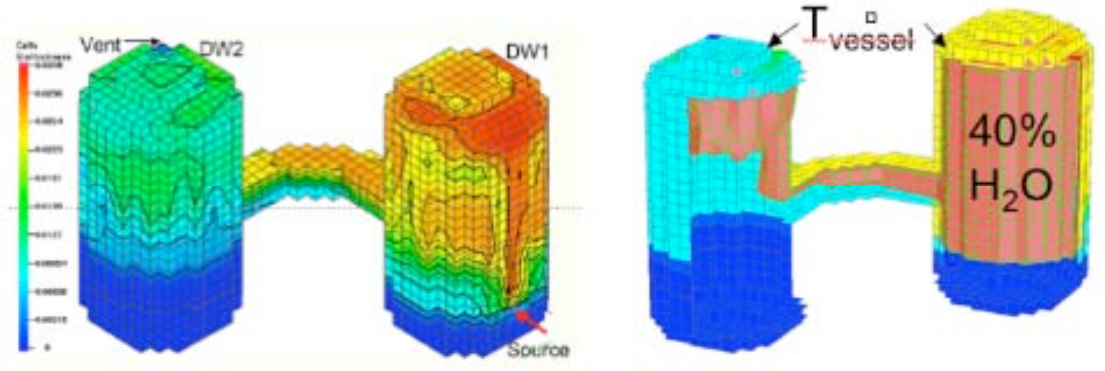

Fig. 6: Test 9bis final condensate film [cm], steam cloud and vessel temperature (7000s)

straight pipe model gives a little more spreading into DW2 with lower concentrations in DW1. The results for the coarse and fine mesh model with the bended connection pipe are

closer. Test 9bis with steam condensation shows higher steam concentrations near the bottom of the facility. They are likely to originate from the vaporization of a draining film into the dry air region below the steam cloud, (Andreani, 2005). GASFLOW only simulates a static film and shows no film in DW2 below the connection pipe in the final snap shot with the coarse 3D model (figure 6) that also gives the 40% steam cloud together with the more elevated vessel temperature in the regions with higher steam concentrations.

The recorded volume flow rates at the vent in DW2 rapidly reduce over the inlet flow to some plateau values that reflect the cooling of the injected steam by mixing with air (figure 7). A

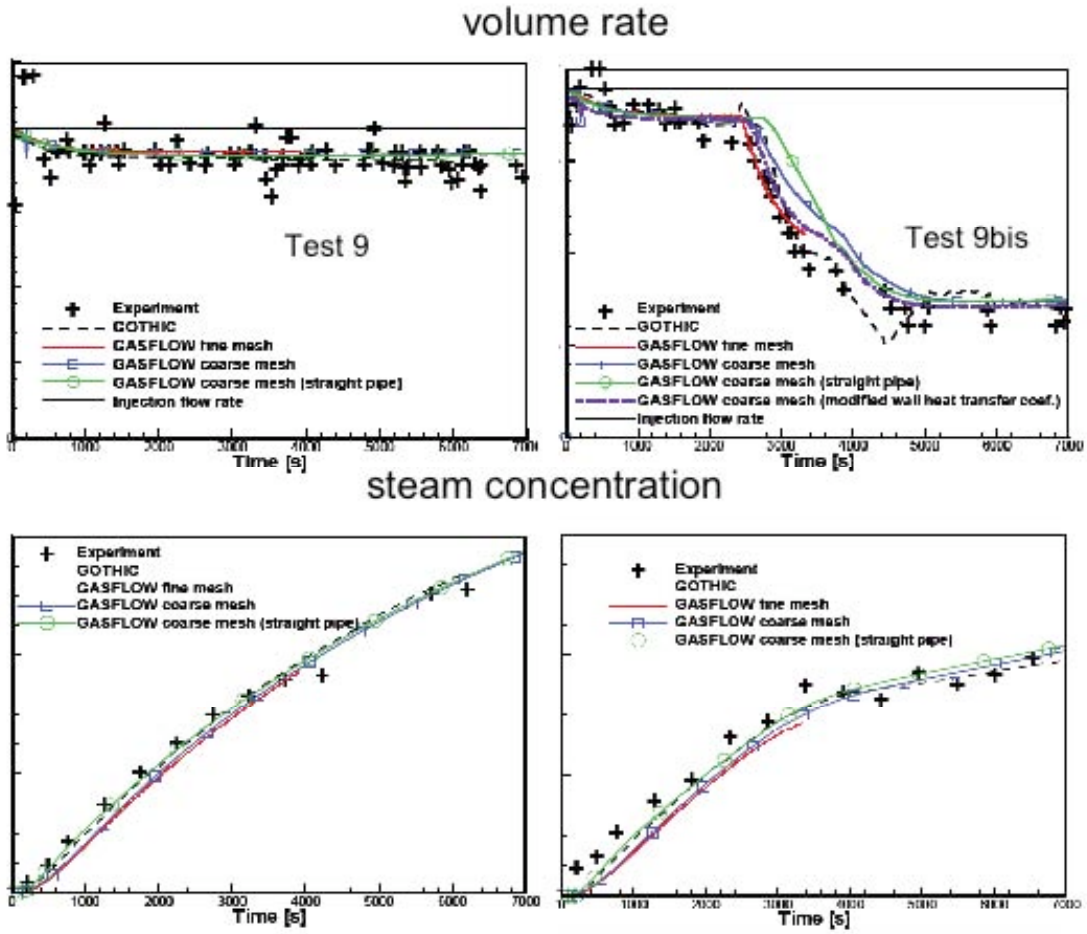

Fig. 7: Volume rate and steam concentration at the vent (tests 9 and 9bis)

further decay to a second plateau occurs in test 9bis after onset of condensation around 3000s. This plateau is controlled by the constant pressure of 1.3 bar at the vent and predicted well. Thermodynamically this pressure enforces a quasi stationary condensation rate with saturated conditions. But the transition to the second plateau is too slow with the coarse model while the fine mesh results follow the test data more closely. The transition in the coarse mesh simulation in which the heat transfer was enhanced by the ratio of the coarse and fine wall mesh (factor 2) falls right on the result of the fine mesh. The measured steam concentration at the vent (lower graph in figure 7) is well predicted in GASFLOW with the coarse and fine meshes It shows similar initial increases and a pronounced slowing down of the growth in test 9bis after condensation onset. Calculated steam distribution in DW1, in the interconnection pipe, and in DW2 show a somewhat better agreement for the coarse models with the bended vs. the straight pipe. But from the tendency both models capture the correct phenomenology.

4.2 Tests 21 and 21bis

The GASFLOW simulation of tests 21 with the straight pipe model also gives excellent predictions for the volume rates and steam concentrations at the vent in DW2 (figure 8) in particular for the time of steam arrival. With the direct impingement of steam in the dome con-

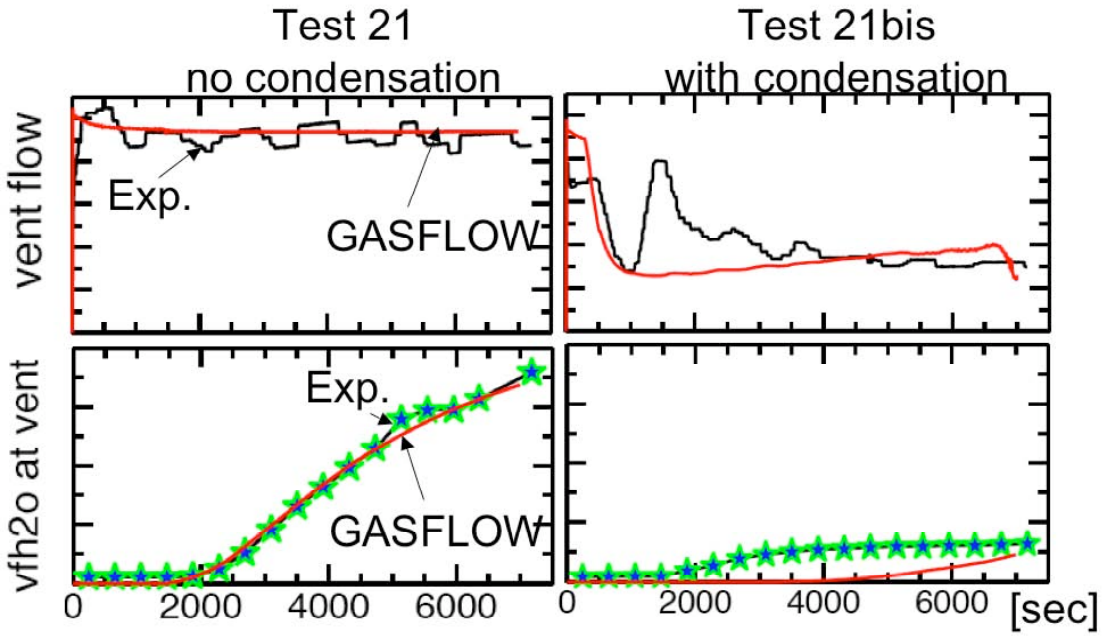

Fig. 8: Volume rate and steam concentration at the vent (test 21 and 21bis)

densation in test 21bis comes in very early and the volume rates reduce more rapidly than in test 9bis. Steam condensation heats up the dome and the volume rate at the vent valve goes through a minimum when the dome structure is saturated and cannot condense so much steam anymore. After this GASFLOW predicts it to rise only gradually as the steam cloud propagates into the vessel regions below the larger dome surface. Initially the test data show a similar behavior but then rise again shortly to an intermediate peak before they decay to similar rates as calculated in GASFLOW. (Andreani, 2007) attributes this peak to an additional volume source from the vaporization of the condensate film draining on the preheated structures into regions with dry air. This interpretation is consistent with the earlier steam arrival in the test relative to the much later arrival predicted in GASFLOW which does not model a moving film. The final steam concentration from GASFLOW at 7000 s approaches the test data well. The quasistationary condensation then reflects the thermodynamic boundary condition set by the vent valve pressure.

4.3 Test 25

The steam/Helium distribution test 25 investigates the distribution of light gas mixtures with condensing steam in air over two rooms with a dead end like it can occur in containment rooms in severe accidents (Royl et al., 2002). Figure 9 gives the applied steam/helium source and the pressure boundary in this test with an axial injection near the mid height of DW1. The initial injection velocity is 4.3 m/s. Injection starts with a Froude number of 2.3 which is characteristic for a rising plume whose buoyancy dominates over the injection momentum already at short distance from the source. The vent is located in the lower region of DW1 far below the injection source and the interconncection pipe (IP). GASFLOW uses a pressure boundary condition at the location of this vent with the recorded monotonic increase of the pressure from figure 9. The source gas is injected from a sealed off reservoir cell in the 3D fluid mesh with a time dependent steam/helium composition using a velocity boundary condi-

tion at the open feeding side on the top of the source cell. GASFLOW has an option to reduce the area of the feeding source cell

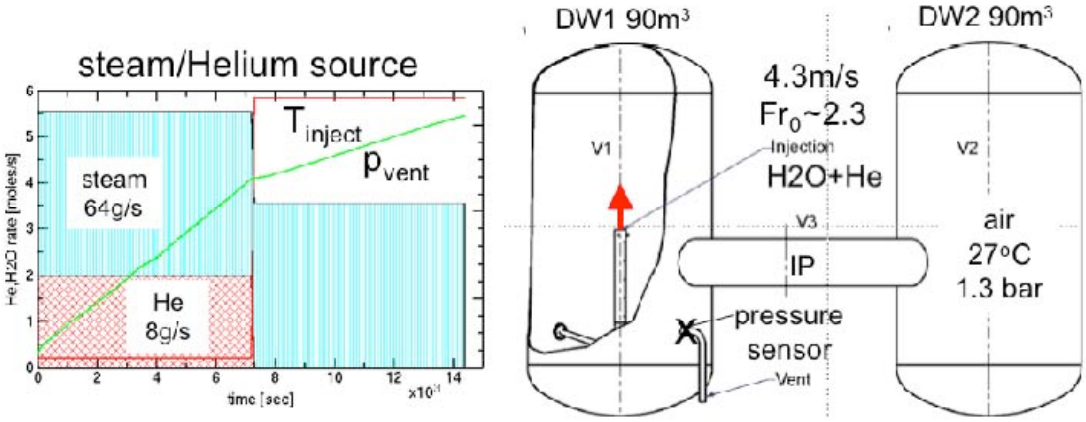

Fig. 9: Source and boundary conditions for test 25

to inject with the correct injection momentum. But the cell surface of 1111 cm2 in the coarse mesh is much larger than the 314 cm2 cross section of the 20 cm injection pipe. The use of this option introduced a too strong air entrainment into the fluid cell right above the source. This diluted the steam/helium mixture close to the source and the concentration of the helium layer built up from steam condensation in the dome did not reach the measured high level. For the buoyancy dominated plume rise in this experiment it turned out better to use the cell face from the coarse mesh without the area reduction and neglect the error from a too low injection momentum.

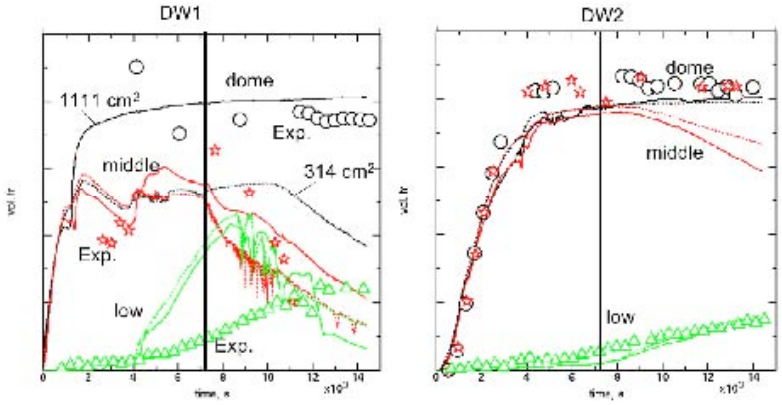

Fig. 10: Helium concentrations DW1 and DW2 in test 25

Figure 10 compares the calculated and measured helium concentrations in the dome, middle and low regions of DW1 and DW2 when using the mesh face of 1111 cm^2 and the reduced area of 314 cm^2. The initial helium volume fraction in the source gas is 36%. As the source plume rises to the dome, steam condenses on the cold vessel which increases the helium volume fraction. More and more helium accumulates in the dome and builds up a stratified high concentration helium layer that isolates itself and prevents the further addition of source gas and energy from below. The stratified layer is not affected at all when the steam/helium/air mixture below flows over into DW2 after 2000 s which temporarily reduces the helium volume fraction in the middle region of DW1. Too much air entrainment due to the local reduction of the cell area prevented the buildup of this layer and gave more mixed concentrations in the middle and upper region of DW1. It also caused a faster increase of the helium concentration in DW2. The gas flowing over into DW2 has already a reduced steam content and nearly all steam that is brought into the cold DW2 condenses. This builds up another low density self insulating high concentration helium layer also in DW2 that is even thicker than in DW1 with almost the same helium concentrations in the dome and middle region. The switch to a pure steam injection after 7200

s has nearly no impact on the stratified layers. They are predicted to remain stable throughout the analysis. The steam only dilutes the helium concentration in the middle region. GASFLOW predictions without the area reduction are in very good agreement with the test data. The temporarily higher than measured concentration predicted in the lower region of DW1 is related to the difficulty to catch the rather sharp lower helium front in phase 1.

The measured concentrations of helium and steam at the vent pipe show helium to arrive 2000 s before any steam reaches this location (figure 11). This earlier arrival of helium far below the injection location is well predicted. It is related to the fact that drying steam/helium/air mixtures on condensing surfaces initially gives locally higher dry air/helium densities and causes a local down flow of the dried helium/air mixture next to the wall. As more and more helium is added the dried steam/helium/air mixtures become lighter. Then they rise and contribute to the stratified gas region. The measured temporary condensation sedimentation effect is of relevance also for containment applications, where increased hydrogen concentrations are eventually predicted in the lower region during most scenarios (Royl et al., 2002) because hydrogen release is limited to lower mixture concentrations than in test 25. Figure 12 gives the regime map in which steam condensation out of a steam/helium/air mixture can result in a sedimentation or stratification depending on the mixture composition. The concentration development during test 25 in a near wall cell has been entered and shows an initial sedimentation phase followed by stratification after the helium/steam concentration crosses the 38/20 % limit. The data from test 25 validate the predicted hydrogen sedimentation that has been questioned in earlier containment applications with GASFLOW. During the steam release after 7200s the helium concentration reduces. The spikes

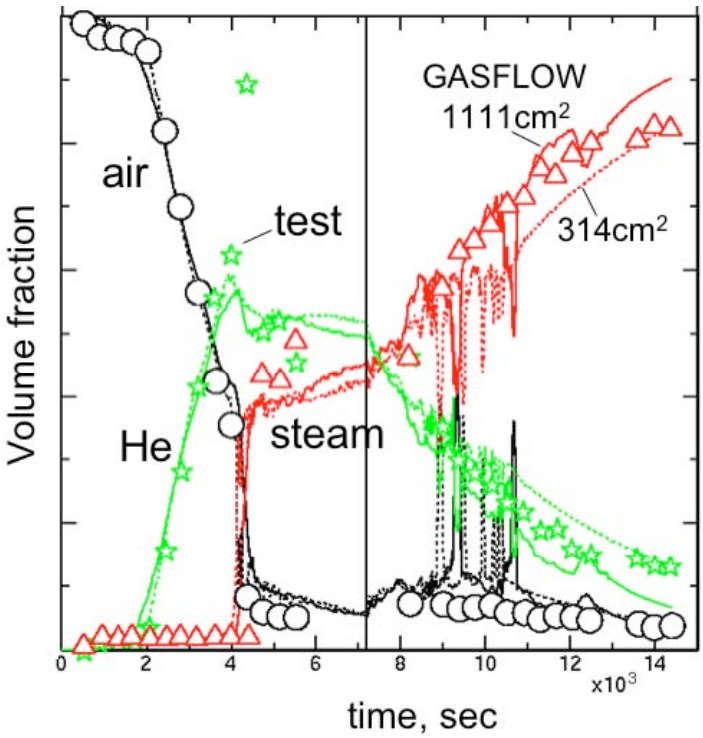

Fig. 11: Gas concentration test 25 at the vent

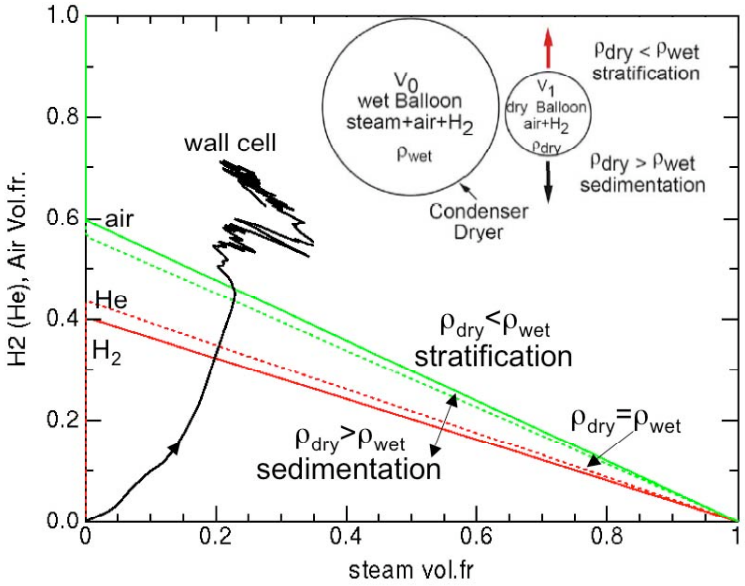

Fig. 12: Thought experiment on density changes from drying steam/he(h2)/air

come from calculated backflows each time when the rising pressure at the vent exceeds the vessel pressure during a short time. The steam released after 7200 s compresses the stratified helium clouds in DW1 and DW2. It cannot penetrate into the clouds with lighter gas, so their temperatures increase only slightly from the compression.

The steam regions in figure 13 under the helium clouds at the top are the zones with the higher fluid temperatures. They are well reflected also in the GASFLOW results. Vessel temperatures in figure 14 also show low values in the region next to the stratified helium cloud in

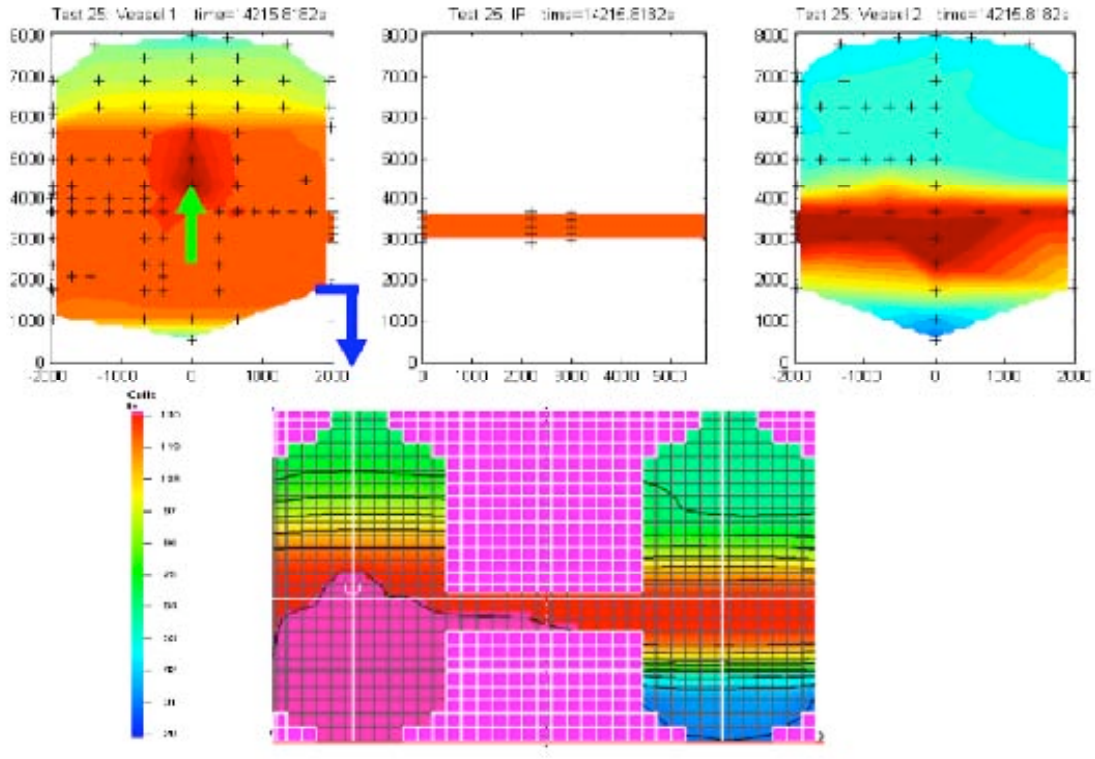

Fig. 13: Final fluid temperatures test 25 at 14400 s

the dome and higher fairly uniform temperatures in the steam cloud underneath. Agreement with the measured data in DW1 is quite good except for the slight increase in the dome region, which is not reflected in the displayed node 28. This GASFLOW node already includes the full heat capacity in the man hole region and cannot follow the temperature increase induced by the gas compression. Figure 14 also shows the applied 3D Cartesian GASFLOW

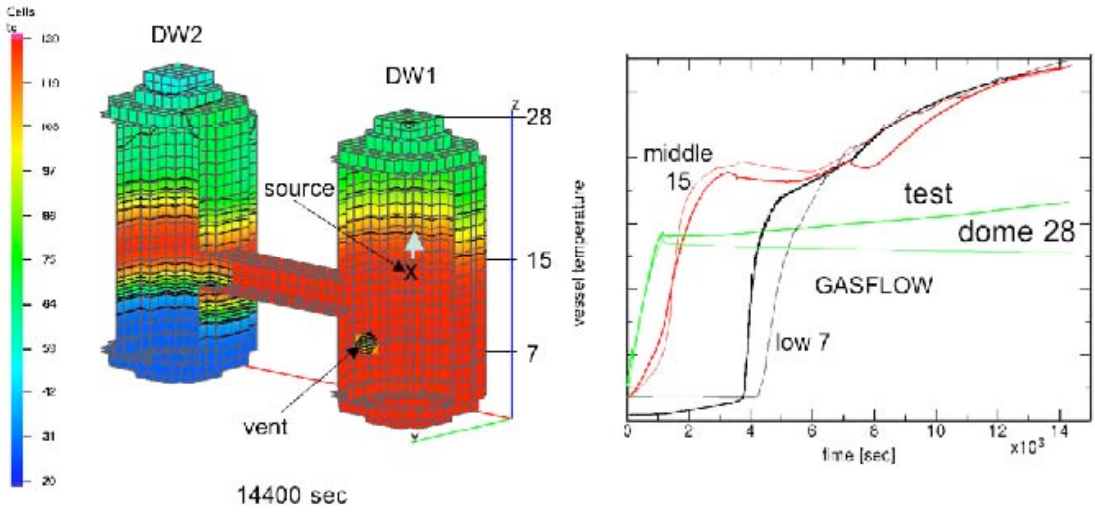

Fig. 14: Final structure temperatures test 25 and test data for DW1

model of the test facility that was simulated adiabatic on the outside as a composite structure with 2 cm steel and 20 cm rockwool assuming 1D heat conduction with 52 nodes. The steel thickness was doubled in the two uppermost nodes due to the thicker structure in the man hole region.

5. CONCLUSIONS

The GASFLOW simulations for the selected Panda tests 9 and 9bis have shown that in the absence of condensation the results with the finest mesh agree well with other calculations for test 9 at the compared reference time of 250s, yet all give higher than measured temperatures. Coarser meshes locally mix mass, momentum and energy too fast, yet globally they give nearly the same results as the fine mesh which holds both for tests 9 and 9bis. Convergence of local data could not be reached with the different meshes. But the successful interpretation of tests 9 and 9bis demonstrates, that broad atmospheric changes can be captured with coarse meshes quite well. Transient locally heterogeneous conditions will not impact much and don't have to be zoomed with extra fine meshes. GASFLOW calculations with coarse meshes for test facilities of widely different sizes (up to full containments like HDR in test E11.2 (Royl et al, 2006)) confirm that one can reliably predict thermal-hydraulic processes in full reactor containments with such models. The failure to properly determine the volume rates at the vent in test 21bis indicates that a moving film model may be a desirable feature for implementation. Both tests 9bis and 21bis are well suited for testing and further improving the steam condensation/vaporization modeling in CFD codes.

Our analysis predicts the high concentration stable helium layers in test 25 quite well in both DW1 and DW2 that result from the steam condensation out of the source gas mixture on the cold vessel walls. This includes a good simulation of helium accumulation in a dead end compartment, like it is found in many reactor containments. The earlier arrival of Helium relative to steam at the vent pipe in test 25 far below the injection source was well predicted. It is related to the fact that steam/helium/air mixtures can temporarily get heavier on condensing walls and give a secondary convection that brings down helium (hydrogen) into the lower region of the containment. As more and more helium is added these dried helium/steam/air layers become lighter and contribute to the stratified gas region. The measured temporary condensation sedimentation effect in test 25 has a big relevance also for containment applications. They exhibit such effect in many scenarios because hydrogen/steam injections never reach high enough hydrogen volume fractions for a condensation stratification. On larger time scales more elevated hydrogen concentrations are thus often accumulated in the lower rather than in the upper containment regions. Test 25 validates this predicted sedimentation effect from containment analyses with GASFLOW that has sometimes been questioned.

The axis scales in the figures of this paper could not be shown to keep confidentiality with respect to the release of these experimental data as addressed in the project agreement. The condensation phenomena controlling this test are relevant for all accident scenarios in reactor containments. Their good interpretation backs up the predictive quality of GASFLOW for full containment simulations. The coarse model applied in the simulation of the facility was sufficient for capturing the dominant phenomena. Using the GASFLOW option to strongly reduce the area of the feeding source cell to match the injection momentum turned out to give too much local entrainment at the source so that this parameter should not be applied to inject with the correct momentum in a coarse mesh. The wall functions to describe heat, mass and momentum transfer in a coarse mesh still require further work to arrive at a heat transfer that is mesh independent when approaching stagnant conditions.

REFERENCES

Andreani, M.:"Comparison between simulations and experiments",
9th Meeting of the Program Review Group OECD SETH project,
Villingen, 19-20 May, 2005

Andreani, M. private communication, 2007

Paladino, D. , R. Zboray, P. Benz, M. Andreani: "Three-Gas-Mixture Plume Inducing Mixing and Stratification in a Multi-Compartment Containment",
Procs NURETH 12, Pittsburg, 2007 #195

Auban, O., Zboray, R., Paladino, D.,"Investigation of Large-scale gas mixing and stratification phenomena related to LWR containment studies in the PANDA facility"
Nuclear Engineering and Design (2006) 2006.07.01

Royl, P., , Rochholz, H., Breitung, W., Travis, J. R., Necker, G.:
"Analysis of steam and hydrogen distributions with PAR mitigation in NPP containments", *Nuclear Engineering and Design 202 (2002) 231-248*

Royl, P. U.J. Lee, J. R. Travis, W. Breitung, "Benchmarking of the 3D CFD Code GASFLOW II with Containment Thermal Hydraulic Tests from HDR and ThAI"
Procs. CFD4NRS Meeting, Munich 2006

Travis et al.: http://www.gasflow.net (2007)

Acknowledgements

Dr. Michele Andreani from the Paul Scherrer Institute, Switzerland contributed to this work and gave many details on all experiments and on their current status of interpretation with other CFD codes. He also shared the results from his GOTHIC analysis of test 25 for comparison and solving of open questions from our analysis. This work was partially funded with a research grant from the brain pool program of the Korean government. The authors are also grateful for the financial support of the participating countries to the joint cooperative SETH project run under the auspices of the Nuclear Energy Agency, Organization for Economic Cooperation and Development.